

Received November 17, 2020, accepted December 1, 2020, date of publication December 7, 2020, date of current version January 28, 2021.

Digital Object Identifier 10.1109/ACCESS.2020.3042808

# OptoNet II: An Advanced MATLAB-Based Toolbox for Functional Cortical Connectivity Analysis With Surrogate Tests Using fNIRS

GIHYOUN LEE<sup>1,2</sup>, JI-SU PARK<sup>3</sup>, JUNGSOO LEE<sup>1</sup>, JINUK KIM<sup>2</sup>,  
YOUNG-JIN JUNG<sup>4</sup>, AND YUN-HEE KIM<sup>1,2</sup>

<sup>1</sup>Department of Physical and Rehabilitation Medicine, Center for Prevention and Rehabilitation, Heart Vascular Stroke Institute, Samsung Medical Center, School of Medicine, Sungkyunkwan University, Seoul 06351, South Korea

<sup>2</sup>Department of Health Sciences and Technology, SAIHST, Sungkyunkwan University, Seoul 06351, South Korea

<sup>3</sup>Advanced Human Resource Development Project Group for Health Care in Aging Friendly Industry, Dongseo University, Busan 47011, South Korea

<sup>4</sup>Department of Radiological Science, Health Sciences Division, Dongseo University, Busan 47011, South Korea

Corresponding authors: Young-Jin Jung (microbme@outlook.com) and Yun-Hee Kim (yun1225.kim@samsung.com)

This work was supported in part by the Korea Health Technology Research and Development Project through the Korea Health Industry Development Institute (KHIDI), funded by the Ministry of Health & Welfare, South Korea, under Grant HI17C1501, and in part by the National Research Foundation of Korea (NRF) grant funded by the Korean Government under Grant NRF-2020R1A2C3010304 and Grant NRF-2019R111A1A01060660.

**ABSTRACT** Cortical connectivity analysis is a widely used method for understanding the causes of neurological disorders and related brain mechanisms. Although there exist numerous activity analysis toolboxes for functional near-infrared spectroscopy (fNIRS), there are only a few cortical connectivity analysis toolboxes. In 2019, we released a MATLAB toolbox named *OptoNet*, which has helped researchers to analyze brain networks using fNIRS. In this study, we developed an advanced MATLAB toolbox, named *OptoNet II*, to add new features that overcome the shortcomings of *OptoNet*. With these new features, *OptoNet II* can efficiently analyze cortical connectivity according to brain region using any fNIRS channel sets and can present the results of two connectivity analyses with auto-thresholding based on surrogate tests. To evaluate the efficacy of the new functions, the finger-tapping task experiment was carried out before and after transcranial direct current stimulation (tDCS) in the primary motor area. *OptoNet II* can efficiently show the effects of tDCS on functional brain region connectivity, which has been difficult to confirm by conventional methods. In this article, we propose the *OptoNet II* as a useful and efficient toolbox for researchers who want to perform cortical connectivity analysis using fNIRS.

**INDEX TERMS** Brain network analysis, brain phase synchronization, cortical hemodynamic signals, cortical connectivity, functional near-infrared spectroscopy.

## I. INTRODUCTION

Functional neural connectivity plays an important role in advanced cognitive processes, and has thus drawn increasing attention from researchers over the past decades [1]–[6]. Various measures, such as phase synchronization index (PSI) [7], mutual information [8], partial directed coherence [9], frequency ratio [10], and mean phase coherence [9], have been applied to quantify the functional connectivity of different brain units using multichannel neural signals, including electroencephalography (EEG), functional magnetic resonance imaging (fMRI), and functional near-infrared spectroscopy

The associate editor coordinating the review of this manuscript and approving it for publication was Poki Chen <sup>1</sup>.

(fNIRS) [5]. These functional connectivity measurements have shown similar global functional connectivity patterns across studies, with some differences between study results for particular cortical regions, and have also shown agreement with regards to quantifying the level of synchronization [2].

fNIRS is a noninvasive method used to measure hemodynamic brain signals based on the absorption of near-infrared light, with wavelengths in the range of 650 nm to 950 nm, transmitted through the intact skull [11]. fNIRS monitors variations in regional cerebral blood flow and estimates hemodynamic signals, which are highly correlated to the blood-oxygenation-level-dependent (BOLD) signal outputs in fMRI [12]. The important advantages of fNIRS are its low cost, portability, and the potential to extend research to a

wider range of environments than many other neuro-imaging systems, such as fMRI, EEG, and magnetoencephalography (MEG) [13].

General linear modeling (GLM) is one of the most extensively used models to represent data in a linear combination form, and constitutes a standard method for analyzing fMRI data. Indeed, many statistical analysis toolboxes have been developed for fNIRS based on the GLM. However, GLM-based analysis methods often fail to adequately analyze brain functions because of artifacts in the fNIRS measurements. The artifacts exist for various reasons, such as subject movements, blood pressure variations, and instrumental instabilities [14]–[19]. Recently, various connection and causality estimation methods for functional brain network analysis have been developed, and have demonstrated their utility in cognitive neuroscience and neurological clinical studies [20]. Many brain network estimation methods have been applied to numerous functional neuroimaging modalities, such as EEG, local field potential, intracranial EEG, MEG, fMRI, and fNIRS.

The most popular tools currently available for fNIRS analysis are hypergeometric optimization of Motif enrichment (HOMER) from Harvard Medical School [21] and near-infrared spectroscopy statistical parametric mapping (NIRS-SPM) from the Korea Advanced Institute of Science and Technology (KAIST) [15]. HOMER (available at <http://www.nmr.mgh.harvard.edu/PMI/>) calculates individual hemodynamic responses using ordinary least-squares linear deconvolution, while NIRS-SPM (available at <http://bisp.kaist.ac.kr/NIRS-SPM>) applies the SPM method, which refers to the construction and assessment of spatially extended statistical processes used to test hypotheses about functional imaging data [3], [15]. However, these analysis tools cannot estimate functional brain connectivity, and they are difficult for new users to learn. Therefore, prior to the release of *OptoNet*, there was no software program for the analysis of functional brain networks using fNIRS available for free and which could be used by unskilled users [3]. In 2019, our research team released a Windows-based graphical user interface (GUI) MATLAB toolbox named *OptoNet* with the aim of providing unexperienced users with an easy way to analyze cortical networks based on 3-dimensional (3D) finite element analysis (FEA) [22], [23]. However, *OptoNet* can only analyze cortical networks for each channel of any given fNIRS system; thus, if the system has many channels, the results of the cortical network analysis can be too complex to check certain networks. Furthermore, *OptoNet* uses a manual threshold setting, which can only show those networks over the user-determined threshold value. This manual threshold setting can cause the objectivity and reliability of the results to be poor.

In this article, we introduce an advanced version of *OptoNet*, named *OptoNet II*, which is also a Windows-based MATLAB toolbox. The primary differences between *OptoNet II* and *OptoNet* are the cortical connectivity analysis according to the functional brain region, the auto threshold

method that uses a surrogate test, and the representation function of the connectivity difference.

In contrast to the previous version of *OptoNet*, users of *OptoNet II* can freely set all fNIRS channels to fit the functional areas of the brain, and therefore analyze cortical connectivity according to functional region. Additionally, *OptoNet II* features an auto-threshold function based on surrogate tests, which can provide significance tests if the original signal has its property randomized among the surrogate data [10]. Detailed descriptions and examples of *OptoNet II* are provided in the following sections. We tested *OptoNet II* using 64-bit Windows 10 installed on Intel i5 and i7 personal computer systems.

## II. METHODS

The procedures of *OptoNet II* can be roughly divided into the following steps: signal processing, brain region model setting, and connectivity analysis. In the fNIRS signal processing step, loading fNIRS data, selecting the fNIRS epoch, and setting the analysis duration are performed. The connectivity processing step consists of loading the standard head model, setting the brain regions, and executing connectivity analysis. The GUI of the toolbox is optimized for the latest version of the MATLAB (ver. R2020a) (MathWorks, Natick, MA, USA) and GeForce (Nvidia, Santa Clara, CA, USA) graphics card series. Figure 1 shows the overall sequential steps and GUI of *OptoNet II*. Next, detailed descriptions for each step will be presented.

### A. SIGNAL PROCESSING STEP

The signal processing step is performed in the signal processing panel of *OptoNet II*. First, the measured fNIRS data can be entered into the “NIRS Data Load” section indicated in Figure 2 A. *OptoNet II* supports the NIR file format, which can be easily converted from the .mat file format of MATLAB. *OptoNet II* also provides an NIRX converter, as shown in Figure 2 B, which can easily convert fNIRS data to .NIR files. The loaded fNIRS signals are plotted, as shown in Figure 2 C, and the plotting type and fNIRS epoch used to analyze connectivity can be set in the “Signal Analysis Section” as shown in Figure 2 D. The processed fNIRS signals are refreshed in the location shown in Figure 2 C; users do not need to execute this procedure more than once unless the fNIRS data or epoch are changed.

### B. BRAIN REGION MODEL SETTING STEP

As seen in Figure 3, the connectivity processing step is performed in the connectivity processing panel. Users can select between the standard and the individual head and cortex models in the “Load Head and Cortex Model” section shown in Figure 3 A. Figure 3 B shows the “Region Analysis” section. If the on/off checkbox is checked, the region analysis mode is activated, while if it remains unchecked, *OptoNet II* is essentially in fNIRS channel-based analysis mode, similar to the original *OptoNet*. Users can set up brain region modeling according to fNIRS channels by inputting information

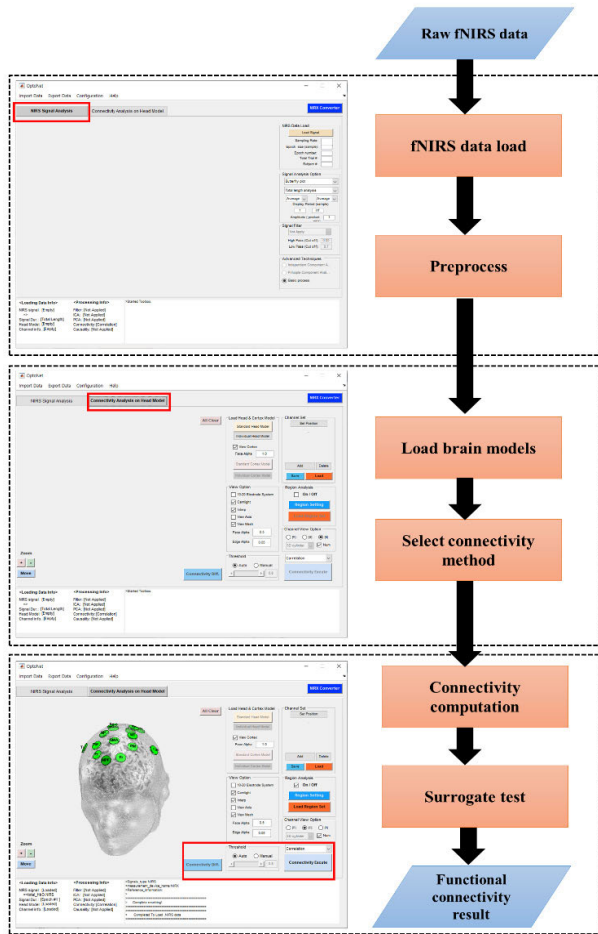


FIGURE 1. Sequential *OptoNet II*.

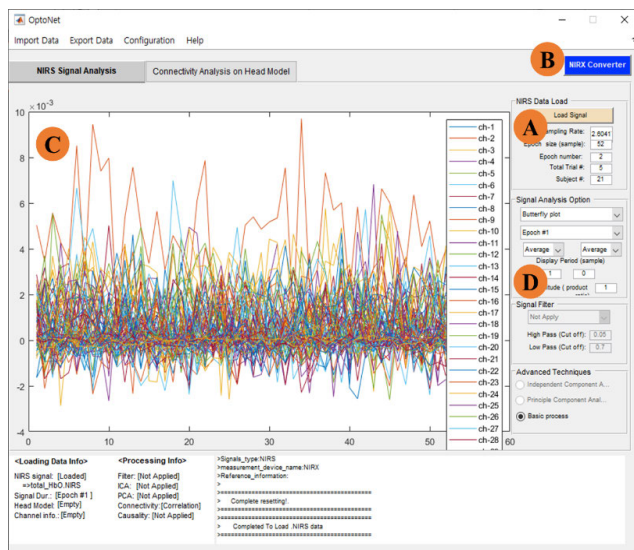


FIGURE 2. The signal processing panel of *OptoNet II*. (A) “NIRS Data Load” section, (B) NIRX converter, (C) “NIRS Signal Plot” section, and (D) “NIRS Signal Analysis” section.

from the fNIRS channels into the “*OptoNet* Region Model Setting” section seen in Figure 3 C. The standard brain region model is separated by 15 regions according to the functional

regions of the brain, including the medial pre-frontal (MPF), the left and right frontal (Lt. Fr and Rt. Fr), the left and right primary motor cortex (Lt. M1 and Rt. M1), supplementary motor area (SMA), the left and right pre-motor cortex (Lt. PM and Rt. PM), the left and right temporal lobe (Lt. Tm and Rt. Tm), the left and right sensory cortex (Lt. Sn and Rt. Sn), the left and right parietal (Lt. Pr and Rt. Pr), and the occipital cortex (Occ).

Once entered, the number of fNIRS channels for each functional region can be saved and used again later. The saved brain region model can be loaded by using the button in Figure 3 B, and then the brain regions that will be analyzed are represented in Figure 3 F. If the user wants to make a custom brain region model that has a different number of functional brain regions from the standard region, the user decides the positions of the region maker on the head model using the position setter in Figure 3 D. Then, custom fNIRS channels are entered as many as the number of the custom regions using the custom region setter that repeats pop-up until pressing the save button in Figure 3 E. The fNIRS channels that are set to the same functional brain region are grouped into that region, and connectivity analysis is performed according to the set brain region model.

C. CONNECTIVITY ANALYSIS STEP

One of the biggest problems that exists when estimating brain connectivity is determining whether corresponding brain region pairs are significantly connected or not with high confidence. The previous version of *OptoNet* only offered the manual threshold setting, which could only represent connections over the manually set threshold; therefore, it could not determine whether there was significant connectivity between regions. In order to overcome this problem, the surrogate data can provide significance tests on whether the original signal has the property randomized among the surrogate data [24], [25]. Therefore, an artificial surrogate test was adopted in this version of *OptoNet II*.

Surrogate methods usually produce artificial data by randomizing the property to be tested while mimicking other properties (e.g., the spectra) of the original signal as much as possible; the more properties that are preserved, the stricter the generated surrogate data [26]. The surrogate time series has the same rank sequence as the Gaussian time series, but the samples of the surrogate time series all come from the measured fNIRS signal. This means that the surrogate series is a rank-shuffled version of the fNIRS signal, with the temporal structure destroyed but the distribution, mean, and variance all preserved [26]. In other words, the surrogate test randomly and independently shuffles fNIRS signals from each cortical source to create a surrogate data set. In order to shuffle fNIRS signals, the phase and amplitude were randomized in the Fourier transformed fNIRS signals to preserve the power spectra feature of measured fNIRS signals with less distortion. Network analysis was estimated from the surrogate data set by performing the same calculating process for 10,000 or more iterations (10,000 times is a default value

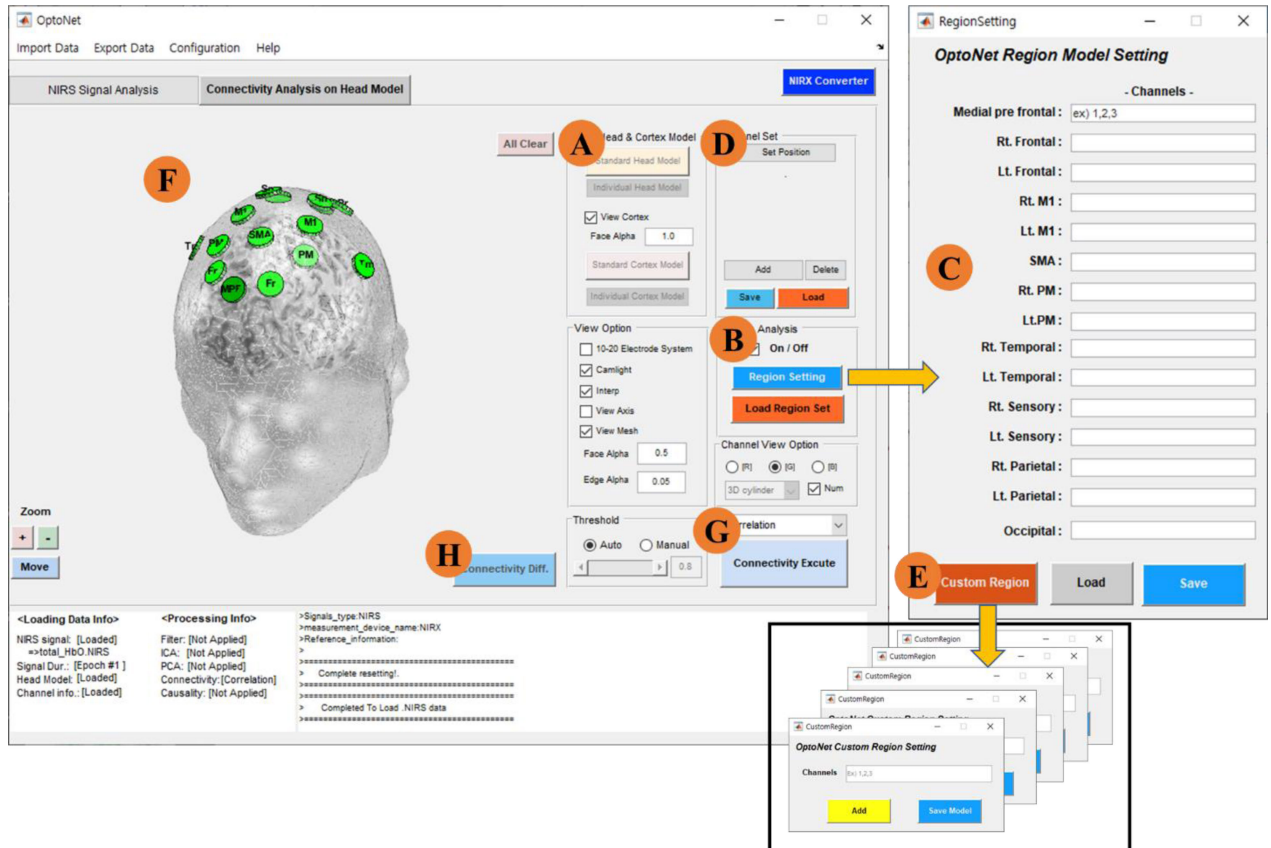


**FIGURE 3.** *OptoNet II* connectivity processing panel. (A) section for selection of the head and cortex models, (B) brain region analysis section, (C) section to input number of fNIRS channels used for each functional brain region, (E) section for threshold selection, connectivity type, and execution of connectivity analysis, and (F) button for analyzing differences in connectivity between datasets.

in the software). In this way, the empirical distribution for a given network estimator can be created. From the distributions, null hypotheses are provided: “the independently and randomly generated surrogate data set has no interactions between generated fNIRS signals”. From these distributions, significant levels for estimated networks were determined from each empirical distribution [2], [27]. The surrogate tests used the auto-threshold method that was added in this new version of *OptoNet II*, and which can be activated using the actions shown in Figure 3 G. To select significant networks, the toolbox follows a rank-order test [28]. First, a residual probability  $\alpha$  of false rejection is selected corresponding to a level of significance  $((1 - \alpha) \times 100\%)$  [25]. Then, for a one-tailed test, which can look for small prediction errors, surrogate sequences ( $M = K/\alpha - 1$ ) are generated, where  $K$  is a positive integer. For a two-tailed test, which can go both ways for time asymmetry, the surrogates ( $M = 2K/\alpha - 1$ ) are generated, resulting in a probability  $\alpha$  that the data gives either one of the  $K$  smallest or largest values [25]. Using more surrogates can increase the discrimination performance [25], and 10,000 surrogate samples were used in *OptoNet II*. If a network has a higher surrogate than the level of significance, it will be represented as a significant network.

The method used for the connectivity analysis can be selected from one of following: correlation [29], [30],

coherence [31], frequency ratio [32], phase locking value (PLV) [33], and is executed as shown in Figure 3 G. After analysis, only significant connectivity is represented in Figure 3 F by auto-thresholding based on the surrogate tests. The resulting values for all estimated connectivities, including insignificant connectivities, are saved in a work folder as a.mat file. If the user wishes to compare two connectivity result files (e.g., rest state and task state), the differences in connectivity can be estimated by using the button shown in Figure 3 H. The difference in the connectivities is calculated through a simple subtraction from the two estimated connectivity results, and then the significant connectivities of the difference are selected using the surrogate test again. After that program is executed, the two results files are continuously loaded and the differences in connectivity between the two files are calculated. Then, the significant differences in connectivity are graphically represented on the head model shown in Figure 3 F.

### III. EXPERIMENTAL RESULTS

We performed an experiment that highlights the improved features of *OptoNet II* over the original version. The experimental task paradigm consisted of the finger tapping task using the left hand.

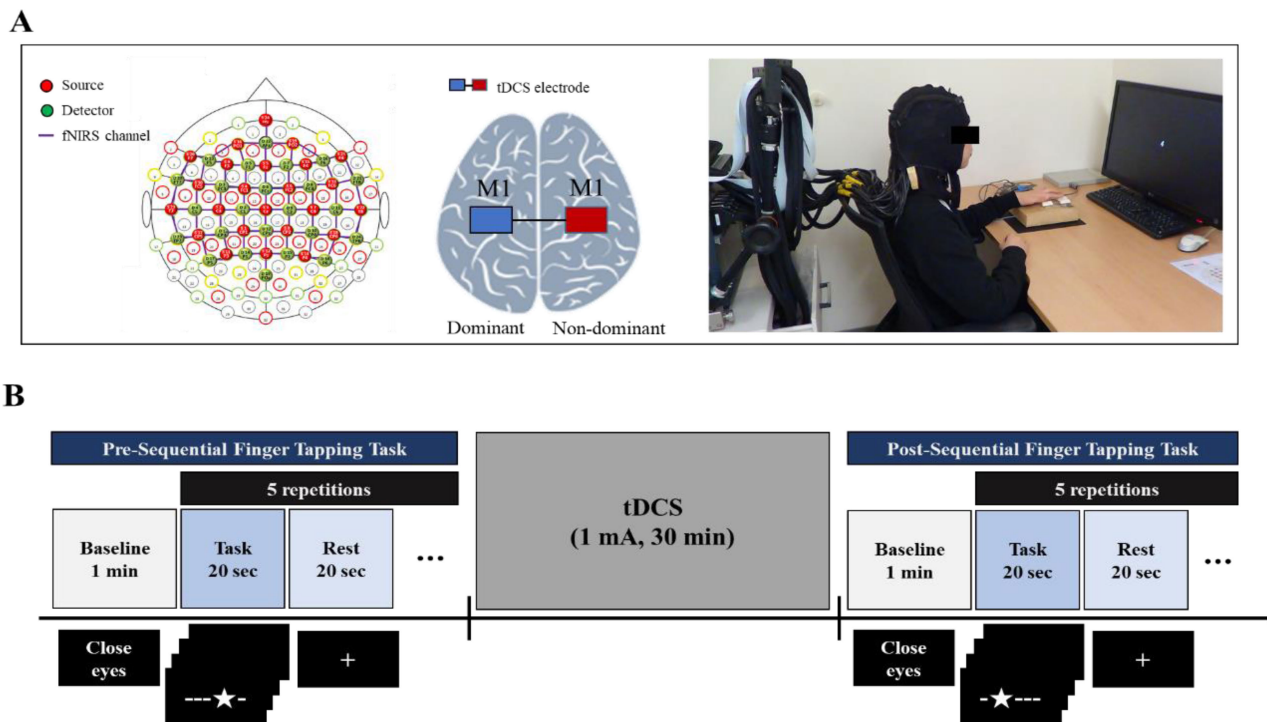


**FIGURE 4.** Experimental conditions (A) structure of fNIRS and tDCS systems and representation of a subject wearing the experimental systems, (B) experimental design and finger tapping task paradigm.

In this experiment, finger tapping is performed sequentially, and participants must accurately tap their finger when prompted by a sign displayed on the monitor screen shown in the right picture in Figure 4 A. Twenty-three adult volunteers over 19 years old who were right-handed were recruited. All subjects were healthy without a history of brain injury, neurological, or psychiatric diseases. Study protocols were approved by the Samsung Medical Center (SMC) Institutional Review Board (IRB), and all subjects gave written informed consent prior to each experiment.

**A. fNIRS SYSTEM**

fNIRS data acquisition was performed with an fNIRS brain imaging system (NIRScout 24-24, NIRx Medizintechnik GmbH, Berlin, Germany). This instrument has a laser near-infrared light source with four wavelengths at 685 nm, 780 nm, 808 nm, and 830 nm. The arrangements of the optode structure and fNIRS channels are shown in Figure 4 A, with 24 NIR sources, 24 NIR detectors, and 81 fNIRS channels. As can be seen in Figure 4 A, the fNIRS channels cover the whole brain cortex in order to analyze cortical connectivity, and it shows the experimental conditions used during fNIRS. fNIRS data were obtained during the pre-sequential finger-tapping task and post-sequential finger tapping task, which have the task block before and after tDCS according to the experimental design in Figure 4 B. The finger-tapping task paradigm starts with the first one-minute eye closed state to obtain a baseline fNIRS signal. The finger-tapping task was performed for 20 seconds with sequentially provided

visual stimulation that permitted a finger press in the same position as the star mark (★). And then, a subject took a rest for 20 seconds and repeated these blocks five times pre- and post-tDCS.

**B. tDCS SYSTEM**

As can be seen in Figure 4 A, the transcranial direct current stimulation (tDCS) electrodes were placed on the scalp, with the anode electrode overlying the right M1 region, which is the area related to the finger-tapping task of the left-hand, that was connected to the cathode electrode overlying the left M1 region. Stimulation was applied using a DC-STIMULATOR (NeuroConn, neuroCare Group, GmbH, Berlin, Germany). The DC current was initially increased in a ramp-like fashion over several seconds (~10 s) until reaching 1 mA, and stimulation was maintained for a total of 30 min. DC currents were turned off slowly over a few seconds, out of the field of view of the patients, a procedure that does not elicit perceived sensations [34].

**C. FUNCTIONAL CONNECTIVITY ANALYSIS**

The sequential finger-tapping task was performed before and after tDCS as shown in Figure 4 B. The experimental block design for the finger tapping task consists of 20-sec task blocks alternating with 20-sec rest blocks to prevent finger fatigue. Five sets of alternating task and rest blocks were performed, and a total of 260 seconds of fNIRS data were acquired, including 1 minute of baseline fNIRS data for twenty-three participants and a total of 115 task blocks.

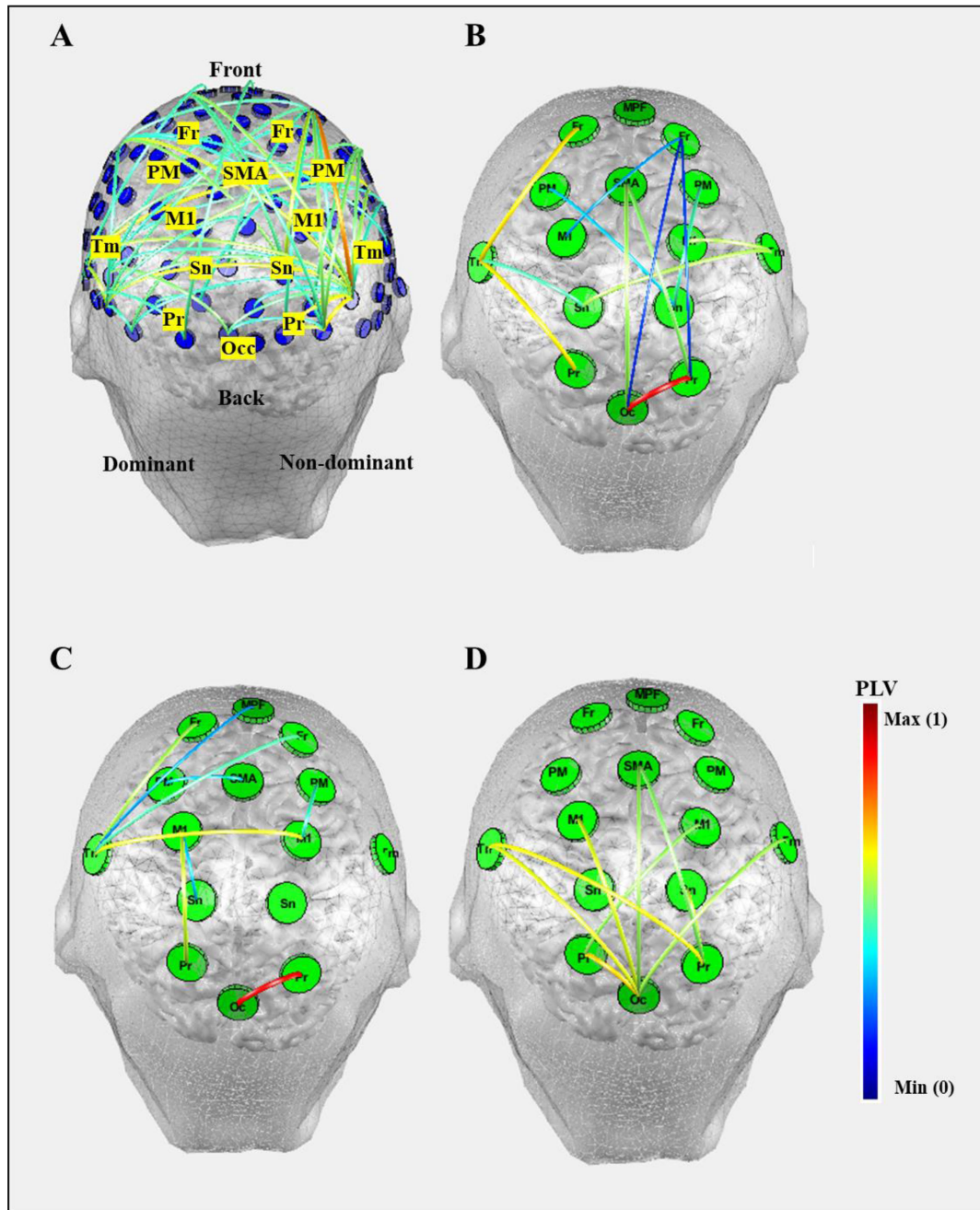


**FIGURE 5.** Functional cortical connectivity, (A) the result from a previous version of *OptoNet*, (B) the result of before tDCS using *OptoNet II*, (C) the result of after tDCS, and (D) the result of the connectivity difference between (C) and (B) using *OptoNet II*.

Estimation of the oxy-hemoglobin (HbO) signal from fNIRS was performed by using the NIRS-SPM toolbox [15] in MATLAB. Band-pass filter and normalization were used as the preprocessing methods for the raw HbO signals. The cutoff frequencies were set between 0.02 ~ 0.1 Hz to remove long-term baseline drifts, high-frequency noise, and cardiac pulsations [35], [36]. And then, band-passed fNIRS data were normalized according to each task block. The fNIRS channels for each functional brain region were selected through

the existing toolbox called fNIRS optodes' location decider (fOLD), which is a first-order approach to bring the advanced parcellation methods and meta-analyses acquired from functional magnetic resonance imaging to more precisely guide the selection of optode positions for fNIRS experiments [37]. The decided fNIRS channels were grouped as follows: MPF (CH 19, 77, 78), Lt. Fr (CH 33, 34, 44), Rt. Fr (CH 72, 73, 74), Lt. M1 (CH 6, 8, 9, 13), Rt. M1 (CH 11, 24, 26, 28), SMA (CH 10, 15, 17, 21), Lt. PM (CH 14, 36), Rt. PM (CH 23, 67),

Lt. Tm (CH 42, 43, 44), Rt. Tm (CH 63, 64, 65), Lt. Sn (CH 2, 3), Rt. Sn (CH 29, 31), Lt. Pr (CH 45, 46, 47), Rt. Pr (CH 51, 52, 53), and Occ (CH 51). In order to avoid signal distortion from differences in the number of fNIRS channels in each group, the fNIRS signals were processed with a narrow band-pass filter and normalization, then they were grouped through ensemble averaging.

Functional connectivity was estimated using the PLV [33], and group analysis for all task blocks of all participants was performed with the use of *OptoNet II* based on estimations using all trials and all epochs, as shown in Figure 5. The functional connectivity results obtained using the original version of *OptoNet* are shown in Figure 5 A, and were obtained based on fNIRS channels with manual thresholding ( $PLV > 0.8$ ). As results for connectivity between functional brain regions cannot be analyzed for significance using the original *OptoNet* due to its fNIRS channel-based analysis and manual thresholding method, the results in Figure 5 A show all connectivity, even insignificant connectivity. Therefore, it is not easy to interpret these results, because there are so many connections among the fNIRS channels.

#### D. CONNECTIVITY ANALYSIS WITH SURROGATE TEST

Figure 5 B, C, and D show the results of connectivity analyses using the new *OptoNet II*. Results concisely presented connectivity between the functional brain regions and showed only connections that were significant using automatic thresholding with the random surrogate tests of 10,000 iterations. Figure 5 B represents the connectivity analysis performed before tDCS, which demonstrated several weak connections spread over wide brain areas between the frontal, temporal, M1, sensory, parietal, and occipital cortices. In particular, the most strong connection was seen between the occipital and parietal areas which can be interpreted as neural activities during the process of performing a motor task using visual cues [34]. Figure 5 C demonstrates the results of post-tDCS connectivity analysis that showed fewer significant connections. Instead, significant new connections were seen between M1, the sensory cortex, and parietal areas following tDCS. This is a result of the changes in the regions related to the motor task and the other associated regions because the brain networks around M1 and sensory cortices are increased after stimulation and the other networks not associated with motor control are decreased after stimulation. This is in line with previous studies, and it is thought that cortical networks begin to work efficiently and form essential connections during a motor task following tDCS [38]–[40]. However, to more clearly identify the difference before and after tDCS, the difference in connectivity before and after stimulation was estimated by using the new toolbox. Figure 5 D shows the differences in connectivity between Figure 5 C and B. As shown here, the significantly stronger connections following tDCS exist between the M1, temporal, parietal, and occipital regions. These are important connections related to the finger-tapping task with attention to a visual stimulus. The connections between the M1s of both

hemispheres and adjacent cortical regions are considered to be the most important brain networks related to the motor task used in this experiment. By using *OptoNet II*, these networks were visualized by calculating the differences in connectivity strength between the pre- and post-tDCS conditions. Therefore, the results of this analysis can support that changes in connectivity between functional brain regions related to the finger tapping task were enhanced following tDCS.

#### IV. DISCUSSION

In 2019, we released a MATLAB toolbox, named *OptoNet*, which can be used to analyze functional cortical networks for fNIRS. It was easy, and simple to use for plotting fNIRS signals and functional cortical connections according to fNIRS channels without any anatomical information. However, if there are many fNIRS channels, it might be difficult for *OptoNet* to find any given important connection due to so many connections.

In order to overcome these issues, we updated *OptoNet* functions. The first updated function is functional brain region-based analysis, which can easily save and load a brain region model after simply entering the number of fNIRS channels, and it can allow for analysis of the connectivity between functional brain region from fNIRS data. The second new capacity is analysis of connectivity differences, which is a function of loading two different saved connectivity results, then representing the different connectivity by task or state between them. We confirmed the clearer effect of tDCS through the connectivity difference between before and after tDCS stimulation. The last new function in *OptoNet II* is random surrogate tests-based auto-thresholding, which allows users to automatically identify only significant connections. The automatic threshold method shows objective meaningful connections by statistical significance through random comparisons of more than 10,000 iterations rather than just a cut off based in simple numerical comparison. Through these updates to *OptoNet II*, we are able to provide much better results reliability to *OptoNet II* users.

In this work, we developed a freely downloadable MATLAB toolbox, named *OptoNet II* (<https://sites.google.com/site/dsucore/free/optonet>) for the analysis of functional cortical connectivity. Any constructive comments and questions are always welcomed through our e-mail.

For future studies, we will update the *OptoNet II* toolbox to have even more user-friendly functions. More methods to evaluate functional connectivity networks to be added include directed transfer function (DTF), Granger causality, transfer entropy, partial directed coherence, and others as programming advances continue. We also plan to enable this toolbox not only for functional network analysis but also for brain activity analysis so that it can be used in all fNIRS research fields.

#### ACKNOWLEDGMENT

(*Young-Jin Jung and Yun-Hee Kim contributed equally to this work.*)

## REFERENCES

- [1] C.-L. Yu, H.-C. Chen, Z.-Y. Yang, and T.-L. Chou, "Multi-time-point analysis: A time course analysis with functional near-infrared spectroscopy," *Behav. Res. Methods*, vol. 52, no. 4, pp. 1700–1713, Feb. 2020.
- [2] G. Lee, J.-S. Park, M. L. B. Ortiz, J.-Y. Hong, S.-H. Paik, S. H. Lee, B. M. Kim, and Y.-J. Jung, "Hemodynamic activity and connectivity of the prefrontal cortex by using functional near-infrared spectroscopy during color-word interference test in Korean and English language," *Brain Sci.*, vol. 10, no. 8, p. 484, Jul. 2020.
- [3] G. Lee, J.-S. Park, and Y.-J. Jung, "OptoNet: A MATLAB-based toolbox for cortical network analyses using functional near-infrared spectroscopy," *Opt. Eng.*, vol. 59, no. 6, p. 1, Oct. 2019.
- [4] P. Pinti, I. Tachtsidis, A. Hamilton, J. Hirsch, C. Aichelburg, S. Gilbert, and P. W. Burgess, "The present and future use of functional near-infrared spectroscopy (fNIRS) for cognitive neuroscience," *Ann. New York Acad. Sci.*, vol. 1464, no. 1, pp. 5–29, Mar. 2020.
- [5] J.-W. Park, G. Lee, B.-M. Kim, Y. Chang, and Y.-J. Jung, "Analytic signal-based causal network estimator for hemodynamic signal analysis in the brain," *J. Korean Phys. Soc.*, vol. 74, no. 9, pp. 847–854, May 2019.
- [6] S. Sutoko, H. Sato, A. Maki, M. Kiguchi, Y. Hirabayashi, H. Atsumori, A. Obata, T. Funane, and T. Katura, "Tutorial on platform for optical topography analysis tools," *Neurophotonics*, vol. 3, no. 1, Jan. 2016, Art. no. 010801.
- [7] D. Rosenbaum, E. J. Leehr, A. Kroczeck, J. A. Rubel, I. Int-Veen, K. Deutsch, M. J. Maier, J. Hudak, A. J. Fallgatter, and A.-C. Ehlis, "Neuronal correlates of spider phobia in a combined fNIRS-EEG study," *Sci. Rep.*, vol. 10, no. 1, pp. 1–14, Dec. 2020.
- [8] K. Takagi, "Principles of mutual information maximization and energy minimization affect the activation patterns of large scale networks in the brain," *Frontiers Comput. Neurosci.*, vol. 13, p. 86, Jan. 2020.
- [9] Q. Zhang, Y. Hu, T. Potter, R. Li, M. Quach, and Y. Zhang, "Establishing functional brain networks using a nonlinear partial directed coherence method to predict epileptic seizures," *J. Neurosci. Methods*, vol. 329, Jan. 2020, Art. no. 108447.
- [10] X. Cheng, Y. Pan, Y. Hu, and Y. Hu, "Coordination elicits synchronous brain activity between co-actors: Frequency ratio matters," *Frontiers Neurosci.*, vol. 13, Oct. 2019.
- [11] A. Villringer and U. Dirnagl, "Coupling of brain activity and cerebral blood flow: Basis of functional neuroimaging," *Cerebrovascular Brain Metabolism Rev.*, vol. 7, no. 3, pp. 240–276, 1995.
- [12] Y. Hoshi, "Functional near-infrared optical imaging: Utility and limitations in human brain mapping," *Psychophysiology*, vol. 40, no. 4, pp. 511–520, Jul. 2003.
- [13] T. Fekete, D. Rubin, J. M. Carlson, and L. R. Mujica-Parodi, "The NIRS analysis package: Noise reduction and statistical inference," *PLoS ONE*, vol. 6, no. 9, Sep. 2011, Art. no. e24322.
- [14] W. Wei, S. Huang, N. Wang, Z. Jin, J. Zhang, and W. Chen, "A near-infrared spectrometer based on novel grating light modulators," *Sensors*, vol. 9, no. 4, pp. 3109–3121, Apr. 2009.
- [15] J. C. Ye, S. Tak, K. E. Jang, J. Jung, and J. Jang, "NIRS-SPM: Statistical parametric mapping for near-infrared spectroscopy," *NeuroImage*, vol. 44, no. 2, pp. 47–428, Jan. 2009.
- [16] K. E. Jang, S. Tak, J. Jung, J. Jang, Y. Jeong, and J. C. Ye, "Wavelet minimum description length detrending for near-infrared spectroscopy," *J. Biomed. Opt.*, vol. 14, no. 3, 2009, Art. no. 034004.
- [17] X. Cui, S. Bray, and A. L. Reiss, "Functional near infrared spectroscopy (NIRS) signal improvement based on negative correlation between oxygenated and deoxygenated hemoglobin dynamics," *NeuroImage*, vol. 49, no. 4, pp. 3039–3046, Feb. 2010.
- [18] G. Lee, S. Jin, and J. An, "Motion artifact correction of multi-measured functional near-infrared spectroscopy signals based on signal reconstruction using an artificial neural network," *Sensors*, vol. 18, no. 9, p. 2957, Sep. 2018.
- [19] G. Lee, S. H. Lee, S. H. Jin, and J. An, "Robust functional near infrared spectroscopy denoising using multiple wavelet shrinkage based on a hemodynamic response model," *J. Near Infr. Spectrosc.*, vol. 26, no. 2, pp. 79–86, Apr. 2018.
- [20] Y.-J. Jung, K. H. Kim, and C.-H. Im, "Mathematical issues in the inference of causal interactions among multichannel neural signals," *J. Appl. Math.*, vol. 2012, pp. 1–14, Jan. 2012.
- [21] T. J. Huppert, S. G. Diamond, M. A. Franceschini, and D. A. Boas, "HomER: A review of time-series analysis methods for near-infrared spectroscopy of the brain," *Appl. Opt.*, vol. 48, no. 10, pp. D280–D298, 2009.
- [22] Y.-J. Jung, J.-H. Kim, and C.-H. Im, "COMETS: A MATLAB toolbox for simulating local electric fields generated by transcranial direct current stimulation (tDCS)," *Biomed. Eng. Lett.*, vol. 3, no. 1, pp. 39–46, Mar. 2013.
- [23] C. Lee, Y.-J. Jung, S. J. Lee, and C.-H. Im, "COMETS2: An advanced MATLAB toolbox for the numerical analysis of electric fields generated by transcranial direct current stimulation," *J. Neurosci. Methods*, vol. 277, pp. 56–62, Feb. 2017.
- [24] M. Palus, "Detecting phase synchronization in noisy systems," *Phys. Lett. A*, vol. 235, no. 4, pp. 341–351, Nov. 1997.
- [25] T. Schreiber and A. Schmitz, "Surrogate time series," *Phys. D, Nonlinear Phenomena*, vol. 142, nos. 3–4, pp. 346–382, Aug. 2000.
- [26] J. Sun, X. Hong, and S. Tong, "Phase synchronization analysis of EEG signals: An evaluation based on surrogate tests," *IEEE Trans. Biomed. Eng.*, vol. 59, no. 8, pp. 2254–2263, Aug. 2012.
- [27] J. S. Kim, C. H. Im, Y. J. Jung, E. Y. Kim, S. K. Lee, and C. K. Chung, "Localization and propagation analysis of ictal source rhythm by electrocorticography," *NeuroImage*, vol. 52, no. 4, pp. 1279–1288, Oct. 2010.
- [28] J. Theiler, S. Eubank, A. Longtin, B. Galdrikian, and J. D. Farmer, "Testing for nonlinearity in time series: The method of surrogate data," *Phys. D, Nonlinear Phenomena*, vol. 58, nos. 1–4, pp. 77–94, Sep. 1992.
- [29] A. Aarabi, F. Wallois, and R. Grebe, "Does spatiotemporal synchronization of EEG change prior to absence seizures?" *Brain Res.*, vol. 1188, pp. 207–221, Jan. 2008.
- [30] G. Thut, D. Veniero, V. Romei, C. Miniussi, P. Schyns, and J. Gross, "Rhythmic TMS causes local entrainment of natural oscillatory signatures," *Current Biol.*, vol. 21, no. 14, pp. 1176–1185, Jul. 2011.
- [31] G. Varotto, E. Visani, S. Franceschetti, G. Sparacino, and F. Panzica, "Spectral and coherence analysis of EEG during intermittent photic stimulation in patients with photosensitive epilepsy," *Int. J. Bioelectromagnetism*, vol. 11, no. 4, pp. 189–193, 2009.
- [32] I. Yilmaz, "Landslide susceptibility mapping using frequency ratio, logistic regression, artificial neural networks and their comparison: A case study from kat landslides (Tokat—Turkey)," *Comput. Geosci.*, vol. 35, no. 6, pp. 1125–1138, Jun. 2009.
- [33] J.-P. Lachaux, E. Rodriguez, J. Martinerie, and F. J. Varela, "Measuring phase synchrony in brain signals," *Hum. Brain Mapping*, vol. 8, no. 4, pp. 194–208, 1999.
- [34] P. C. Gandiga, F. C. Hummel, and L. G. Cohen, "Transcranial DC stimulation (tDCS): A tool for double-blind sham-controlled clinical studies in brain stimulation," *Clin. Neurophysiol.*, vol. 117, no. 4, pp. 845–850, Apr. 2006.
- [35] F. S. Racz, P. Mukli, Z. Nagy, and A. Eke, "Increased prefrontal cortex connectivity during cognitive challenge assessed by fNIRS imaging," *Biomed. Opt. Exp.*, vol. 8, no. 8, pp. 3842–3855, 2017.
- [36] S. Ge, Q. Yang, R. Wang, P. Lin, J. Gao, Y. Leng, Y. Yang, and H. Wang, "A brain-computer interface based on a few-channel EEG-fNIRS bimodal system," *IEEE Access*, vol. 5, pp. 208–218, 2017.
- [37] G. A. Zimeo Morais, J. B. Balardin, and J. R. Sato, "fNIRS Optodes' location decider (FOLD): A toolbox for probe arrangement guided by brain regions-of-interest," *Sci. Rep.*, vol. 8, no. 1, pp. 1–11, Dec. 2018.
- [38] R. Polania, M. A. Nitsche, and W. Paulus, "Modulating functional connectivity patterns and topological functional organization of the human brain with transcranial direct current stimulation," *Hum. Brain Mapping*, vol. 32, no. 8, pp. 1236–1249, Aug. 2011.
- [39] A. Antal, R. Polania, C. Schmidt-Samoa, P. Dechent, and W. Paulus, "Transcranial direct current stimulation over the primary motor cortex during fMRI," *NeuroImage*, vol. 55, no. 2, pp. 590–596, Mar. 2011.
- [40] J. Baudewig, M. A. Nitsche, W. Paulus, and J. Frahm, "Regional modulation of BOLD MRI responses to human sensorimotor activation by transcranial direct current stimulation," *Magn. Reson. Med.*, vol. 45, no. 2, pp. 196–201, 2001.

**GIHYOUN LEE** received the B.S., M.S., and Ph.D. degrees from Kyungpook National University (KNU), in 2009, 2012, and 2016, respectively. He was with the Daegu Gyeongbuk Institute of Science & Technology (DGIST), from August 2016 to August 2018, and also with the Institute of Biomedical Engineering Research, KNU, from September 2019 to February 2019. He joined the Department of Physical and Rehabilitation Medicine, Center for Prevention and Rehabilitation, Heart Vascular Stroke Institute, in March 2019. He is currently a Senior Researcher with the Samsung Medical Center and also a Postdoctoral Researcher with Sungkyunkwan University. His research interests include brain network analysis, neural networks, artificial intelligence, machine learning, brain signal processing, and brain activation mapping.



**JI-SU PARK** received the Ph.D. degree from the Department of Rehabilitation Science, Inje University, Gimhae, South Korea, in 2018. He is currently a Research Professor with the Advanced Human Resource Development Project Group for Health Care in Aging Friendly Industry, Dongseo University, South Korea. His research interests include stroke rehabilitation, neuromodulation, and dysphagia rehabilitation.

**JUNGSOO LEE** received the B.S. degree in electrical engineering and computer science from Kyungpook National University, Daegu, South Korea, in 2010, and the M.S. and Ph.D. degrees in electrical engineering from the Korea Advanced Institute of Science and Technology, Daejeon, South Korea, in 2012 and 2017, respectively. He is currently a Research Professor with the Samsung Medical Center, School of Medicine, Sungkyunkwan University, Seoul, South Korea. His research interests include neuroimaging for predicting a recovery in stroke patients and noninvasive brain stimulation for improving their functions.

**JINUK KIM** received the B.S. and M.S. degrees in mechanical and control engineering from Handong Global University, Pohang, South Korea, in 2015 and 2017, respectively. He is currently pursuing the Ph.D. degree in health sciences and technology with Sungkyunkwan University, Seoul, South Korea. His research interests include neurorehabilitation and neuroimaging analysis.

**YOUNG-JIN JUNG** received the Ph.D. degree from Yonsei University. He was a Research assistant Professor with Hanyang University in 2011. In January 2012, he was with the Department of Biomedical Engineering, Florida International University, USA as a Postdoctoral Associate. Then, he promoted as an Assistant Professor with the College of Nursing and Health Science, Florida International University. He is currently an Assistant Professor with the Department of Radiological Science, Dongseo University, South Korea. He has published more than 35 articles in reputed journals (H-index = 11, google scholar). His current research interests include computational radiological engineering, especially, imaging processing and reconstruction in neuroimaging & neurorehabilitation.

**YUN-HEE KIM** is currently a Professor with the Department of Physical and Rehabilitation Medicine and serves as the Director for the Center for Prevention and Rehabilitation, Heart Vascular Stroke Institute, Samsung Medical Center, School of Medicine, Sungkyunkwan University, Seoul, South Korea. Her clinical specialty is neurological rehabilitation for patients with brain disease. She has authored more than 260 peer-reviewed articles and ten book chapters in the field of neurologic rehabilitation. Her current research interests include human neural plasticity using functional neuroimaging, noninvasive brain stimulation such as transcranial magnetic or direct current stimulations, and rehabilitation robotics. She is the President of the Korean Society for Neurorehabilitation and also holds other leadership positions in other Korean academic societies.

• • •